Direct Access to Thermodynamics from Equilibrium Compositional Heterogeneities

Diego Moreno Martinez

CEA, DES, ISEC, DMRC, Univ Montpellier, Marcoule, France

Email: diego.morenomartinez@cea.fr

1. Force Field parameters and simulation preparation

For the n-dodecane molecules and TBP molecules parameters were taken from gaff2 force field.[1] The dihedral parameters developed by Junmei et al.[2] were used for aliphatic chains (n-dodecane and TBP molecules). The OPLS-AA parameters were used for non-bonded interactions of aliphatic chains of both n-dodecane and TBP molecules.[3] The used water model was the OPC model.[4] The atomic partial charges of the TBP molecules have been calculated using the RESP fitting of the electrostatic potentials,[5] from HF/6-31G* calculations (see Figure S.I.1), which is the recommended level of theory for non-polarizable MD simulations, using Gaussian09.[6]

The boxes were generated using the packmol program.[7] The quantity of molecules placed in the boxes (see Table S.I.1) was calculated in order to obtain, after pressure equilibration, box dimensions close to 70·70·400 Å^3. The initial position were distributed such as the organic phase was placed in the center of the box, surrounded by the aqueous phase (same number of water molecules on each side, see Figure S.I.2). The simulations were prepared in order to attain equilibrium by diffusion of water intro the organic phase. Periodic boundary conditions were

applied to the simulation boxes and a 12 Å truncation cutoff was used for the Lennard-Jones potential truncation. The electrostatic interactions have been calculated using the particle-mesh Ewald method with a similar cutoff of 12 Å.[8] A 2 fs time step was used to integrate the equations of motion and the hydrogen atoms were kept frozen by SHAKE algorithm.[9]

The MD boxes were equilibrated in the NPT ensemble at 1 atm and 300 K maintained constant with a Berendsen barostat and a weak-coupling thermostat.[10] Once the equilibration done, the production runs were performed in the NVT ensemble using the same thermostat. The Berendsen thermostat and barostat were employed to ensure stable equilibration and density stabilization of the large biphasic systems considered in the present work. Since the present analysis focuses primarily on equilibrium concentration profiles rather than fluctuation amplitudes or dynamical properties, the qualitative thermodynamic relationship reported here is not expected to depend critically on the precise thermostat/barostat choice.

The MD trajectories were analyzed using cpptraj package from Amber20 program. All the z profiles were calculated using a Δz resolution of 0.25 Å. For clarity, only one interface is shown in the analysis. The profiles were obtained by averaging the two interfaces present in the simulation box with respect to the symmetry plane located at the center of the organic phase.

	N° of H_2O molecules	N° of TBP molecules	N° of n-dodecane molecules	Box dimensions (Å) (Volume in Å^3)
Diluted B contacted to pure A	33120	812	1662	L_x : 70.69 L_y : 70.69 L_z : 399.88 ($1.998231 \cdot 10^6$ Å^3)
Pure B contacted to Pure A	33120	2199	0	L_x : 70.45 L_y : 70.45

				L_z : 398.73 ($1.978978 \cdot 10^6$ Å^3)

Table S.I.1. Composition and dimensions of box simulations boxes

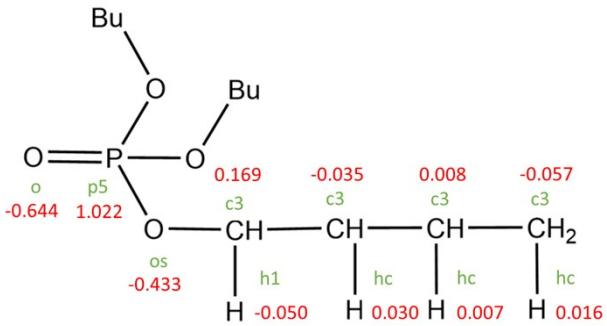

Figure S.I.1. Partial Charges and atom-type of the TBP molecule.

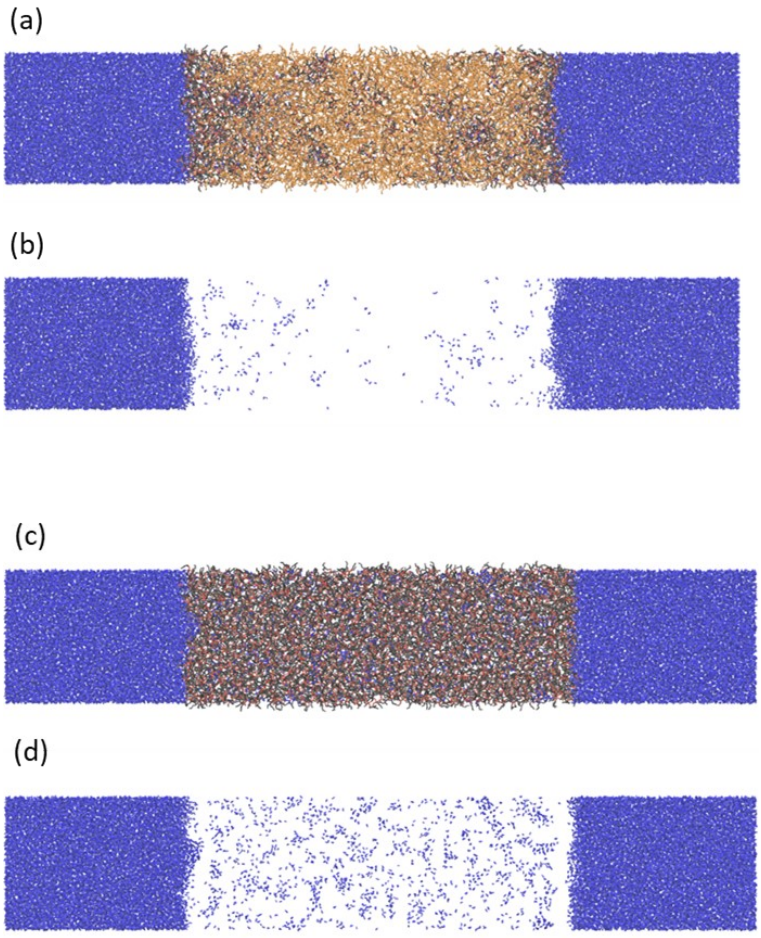

Figure S.I.2. Snapshots of the simulated systems. (a) Snapshot containing all components in the simulation of diluted B contacted to pure A (water, n-dodecane and TBP molecules). (b) The simulation box where only water molecules (species A) are shown for sake of clarity. (c) Snapshot containing all components in the simulation of pure B contacted to pure A (water and TBP molecules). (d) The simulation box where only water molecules (species A) are shown for sake of clarity. Water and n-dodecane molecules are shown in blue and orange color respectively. For TBP molecules, oxygen, phosphorous and carbon atoms are shown in red, tan and black. The aliphatic hydrogen atoms are not shown for more clarity.

2. Equilibrium characterization

The equilibrium was reached when the amount of water molecules in the organic phase remains, in average, constant. Figure S.I.3 shows the evolution of the number of water molecules in the organic phase (excluding the interfacial region). A plateau can be discerned in both simulations. It is noteworthy that this plateau contains fluctuations due to the constant dynamic exchange of water molecules between the two phases. The main simulation (diluted B contacted to pure A) was run up to 8 μs to ensure sufficient sampling of the phase space. The simulation of pure B contacted to pure A was ran for 5 μs. Interestingly, sporadic excursions of species B were observed into the aqueous phase in both simulations (see Figure S.I.4). The solubility of B in water being very low, these excursions are not usually observed in nanoseconds simulations, underlining the extensive sampling of the simulations. The electrostatic profile of the simulations can be also observed in Figure S.I.5.

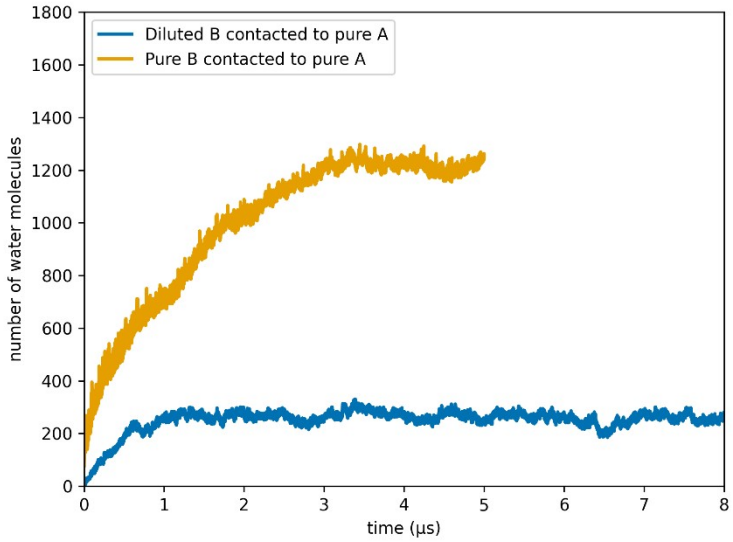

Figure S.I.3. Number of water molecules in the organic phase through time.

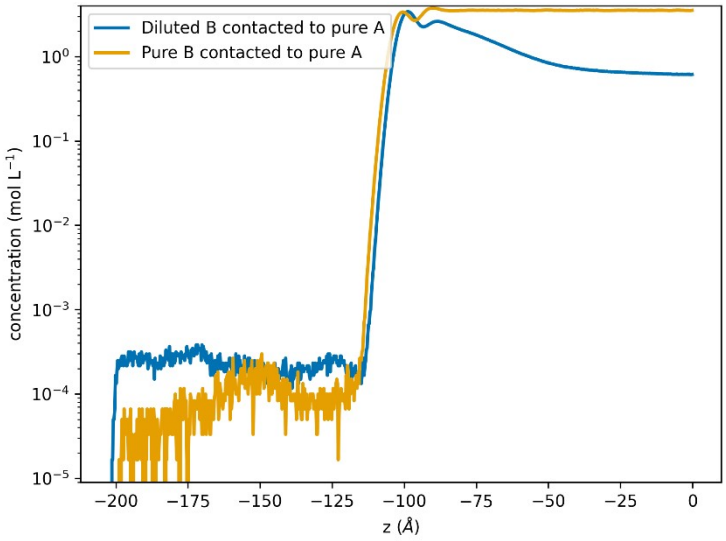

Figure S.I.4. Concentration profiles of B species in log scale.

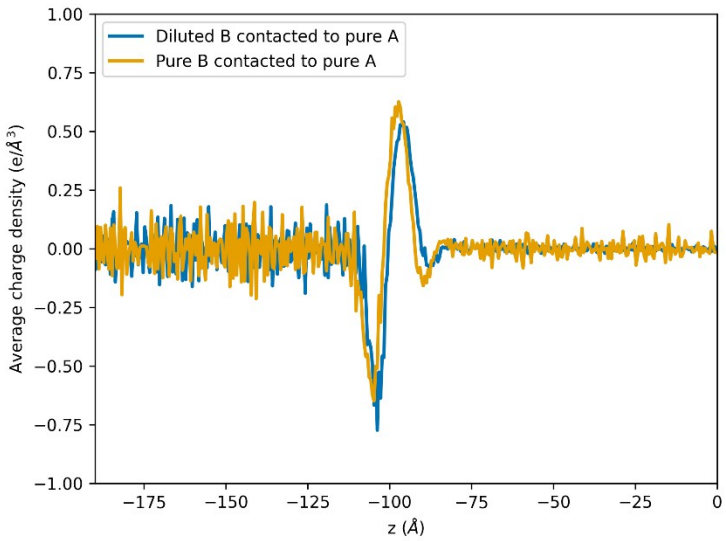

Figure S.I.5. Average charge density along *z* axis.

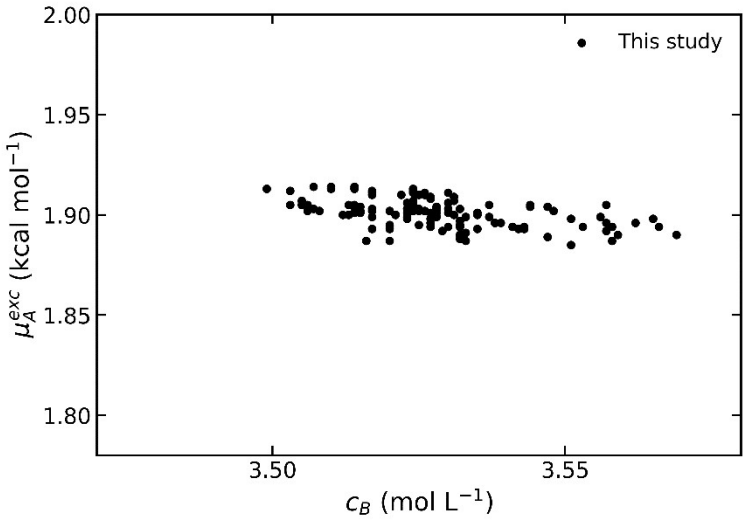

Figure S.I.6. Excess chemical potential of A (μ_A^{exc}) as a function of the concentration of B (c_B) in the case of a pure phase of B contacted to a pure phase of A. Here the distribution of the data is obtained from, as detailed in the main text, concentration and excess chemical potential fluctuations in the bulk organic phase.

3. Excess Chemical Potential from Density of Probability

3.1 Determination of the Local Excess Chemical Potential from Equilibrium Profiles

At thermodynamic equilibrium, the chemical potential of species A is equal in the two coexisting phases:

$$\mu_A^{aq} = \mu_A^{org}$$

More generally, in an inhomogeneous system at equilibrium, the chemical potential remains constant throughout space:

$$\mu_A(z) = \mu_A^{bulk}$$

The chemical potential can be decomposed into ideal and excess contributions:

$$\mu_A(z) = \mu_A^{id}(z) + \mu_A^{exc}(z)$$

The ideal contribution is related to the local number density:

$$\mu_A^{id}(z) = K_B T \, ln\rho_A(z)$$

Thus:

$$\mu_A^{exc}(z) = \mu_A^{bulk} - K_B T \, ln\rho_A(z)$$

Taking a reference bulk region (e.g., the aqueous phase), one obtains:

$$\mu_A^{exc}(z) - \mu_A^{exc,aq} = - K_B T \, ln\left(\frac{\rho_A(z)}{\rho_A^{aq}}\right)$$

This expression shows that the spatial variation of the local density directly reflects variations in the excess chemical potential relative to a bulk reference.

3.2 Relation to the Potential of Mean Force

The potential of mean force (PMF) along the z-coordinate is defined from the equilibrium probability density $P_A(z)$:

$$W_A(z) = - K_B T \ln P_A(z) + C$$

Since $P_A(z) \propto \rho_A(z)$, it follows that:

$W_A(z) = -K_B T \ln \rho_A(z) + C'$

Combining with the previous expression yields:

$W_A(z) = \mu_A^{exc}(z) + constant$

Thus, up to an additive constant, the PMF corresponds to the local excess chemical potential.

3.3 Final Expression

By choosing a bulk reference, the constant can be removed:

$$\mu_A^{exc}(z) = -K_B T \, ln\left(\frac{\rho_A(z)}{\rho_A^{aq}}\right)$$

3.4 Distribution coefficient

It can be shown that the distribution coefficient can be obtained by the following expression:

$$D = K\left(\frac{C_B}{c^\circ}\right)^\alpha$$

With

$$K = \left(\frac{\mu_{A,aq}^{exc} - \mu_{A,org}^{exc}}{K_B T}\right)$$

4. References

(1) Wang, J.; Wolf, R. M.; Caldwell, J. W.; Kollman, P. A.; Case, D. A. Development and Testing of a General Amber Force Field. *J. Comput. Chem.* **2004**, *25* (9), 1157–1174. https://doi.org/10.1002/jcc.20035.

(2) Wang, J.; Kollman, P. A. Automatic parameterization of force field by systematic search and genetic algorithms. *Journal of Computational Chemistry* **2001**, *22* (12), 1219–1228. https://doi.org/10.1002/jcc.1079.

(3) Siu, S. W. I.; Pluhackova, K.; Böckmann, R. A. Optimization of the OPLS-AA Force Field for Long Hydrocarbons. *J. Chem. Theory Comput.* **2012**, *8* (4), 1459–1470. https://doi.org/10.1021/ct200908r.

(4) Izadi, S.; Anandakrishnan, R.; Onufriev, A. V. Building Water Models: A Different Approach. *J. Phys. Chem. Lett.* **2014**, *5* (21), 3863–3871. https://doi.org/10.1021/jz501780a.
(5) Bayly, C. I.; Cieplak, P.; Cornell, W.; Kollman, P. A. A Well-Behaved Electrostatic Potential Based Method Using Charge Restraints for Deriving Atomic Charges: The RESP Model. *J. Phys. Chem.* **1993**, *97* (40), 10269–10280. https://doi.org/10.1021/j100142a004.
(6) Frisch; MJEA and Trucks; GW and Schlegel; H Bernhard and Scuseria; Gustavo E and Robb; Michael A and Cheeseman; James R and Scalmani; Giovanni and Barone; Vincenzo and Mennucci; Benedetta and Petersson; GAea and others. Gaussian 09, Revision d. 01, Gaussian. *Inc., Wallingford CT*. 2009.
(7) Martínez, L.; Andrade, R.; Birgin, E. G.; Martínez, J. M. PACKMOL: A package for building initial configurations for molecular dynamics simulations. *Journal of Computational Chemistry* **2009**, *30* (13), 2157–2164. https://doi.org/10.1002/jcc.21224.
(8) Darden, T.; York, D.; Pedersen, L. Particle Mesh Ewald: An N·log(N) Method for Ewald Sums in Large Systems. *J. Chem. Phys.* **1993**, *98* (12), 10089–10092. https://doi.org/10.1063/1.464397.
(9) Ryckaert, J.-P.; Ciccotti, G.; Berendsen, H. J. C. Numerical Integration of the Cartesian Equations of Motion of a System with Constraints: Molecular Dynamics of n-Alkanes. *J. Comput. Phys.* **1977**, *23* (3), 327–341. https://doi.org/10.1016/0021-9991(77)90098-5.
(10) Berendsen, H. J. C.; Postma, J. P. M.; van Gunsteren, W. F.; DiNola, A.; Haak, J. R. Molecular Dynamics with Coupling to an External Bath. *J. Chem. Phys.* **1984**, *81* (8), 3684–3690. https://doi.org/10.1063/1.448118.